Polymer 50 (2009) 5314–5325

Contents lists available at ScienceDirect

Polymer

journal homepage: www.elsevier.com/locate/polymer

Theoretical investigation of polymers near surface of various molecular weights, architecture and external parameters by mean-field variable-density model

Georgios Kritikos [a], Andreas F. Terzis [a,b,*]

[a] Department of Physics, School of Natural Sciences, University of Patras, Rion, GR-26504 Patras, Greece
[b] Department of Physics, University of Cyprus, 1678 Nicosia, Cyprus

ARTICLE INFO

Article history:
Received 29 March 2009
Received in revised form
9 September 2009
Accepted 9 September 2009
Available online 15 September 2009

Keywords:
Polypropylene
Polymer near surface and polymer brush
Self-consistent mean-field method

ABSTRACT

We extend our recently developed numerical self-consistent mean-field method in order to investigate polydisperse polymer near surfaces and polymer brushes of variable density in the interfacial region. The system studied is melt polypropylene of various architectures (linear or star) and various molecular weights (monodisperse or polydisperse) under constant external pressure. Our main goal is to systematically study the mechanical properties of interfacial systems between solid surfaces and polymer melts. The mechanical properties and especially the fracture dynamics are investigated by a kinetic Monte Carlo simulation. The findings are supported and compared to several structural properties of the macromolecular interfacial system. Our results are in accordance to expected behavior and experimental data.

1. Introduction

Polymers are macromolecular structures that play important role in science and engineering. Although their behavior in the bulk is well studied for several decades their properties near surfaces is the subject of several experimental and theoretical investigation in the last two decades. Actually, in the recent years there is a lot of progress in the field of polymer adsorption at liquid interfaces and solid surfaces, which has been reported in many excellent books [1] and review articles [2]. Strong overlap among neighboring chains adsorbed on a surface is observed once the average distance between the projections of the center of mass of the polymer chain on the surface is small compared to the macromolecular chain dimensions. In this case, the chains deform and stretch in the direction perpendicular to the interface, forming what is usually called (polymer) brush [3].

The polymers near surface and the macromolecular brushes have been studies theoretically in the context of statistical mechanics. These studies include theoretical models of the Landau–Ginzburg free energy functional type [4] or of the path integral form [5]. Moreover, several mean-field theories exist on the discrete (lattice) space [6,7] and continuous space [8,9]. Finally, a considerable amount of theoretical research exists relied on the numerical tool of (statistical mechanical) molecular simulations [10–12].

The numerical tool of the (self-consistent) mean-field theory on a lattice is a powerful method that can describe well polymer near surfaces and polymer brushes. The discrete space used in this approach allows us to reduce the number of chain conformations while the introduction of stiffness promotes the more realistic ones. This mean-field lattice model is much cheaper than experimental and molecular simulation techniques and can guide the production and research for polymers of very complicated architecture, very high molecular weight and under extreme external conditions (for example temperature and pressure). In this work we have developed a lattice-based numerical self-consistent field method in order to describe variable-density polymeric systems next to surfaces or in case of mixtures their interfacial region. In the present article we have focused our studies in (homopolymer) polypropylene. We have studied several architectures (linear and star-like). The molecular weight is another parameter of the system. We assume various values of monodisperse and polydisperse systems. Finally, the effect of the applied external pressure is systematically investigated.

The presentation is described in three more sections. In Section 2 we give the theoretical formulation and mapping of realistic chains onto the lattice and the needed adjustments for the description of the variable density per layer. In Section 3 present the systematic theoretical results and discuss our findings. Finally, in the last section we end our presentation with conclusions and proposals for future studies.

* Corresponding author. Department of Physics, School of Natural Sciences, University of Patras, Rion, GR-26504 Patras, Greece. Tel./fax: +30 2610 996099.
E-mail addresses: terzis@physics.upatras.gr, afterzis@upatras.gr (A.F. Terzis).

0032-3861/$ – see front matter © 2009 Elsevier Ltd. All rights reserved.
doi:10.1016/j.polymer.2009.09.030

2. Theoretical formulation

The theoretical model used to describe the variable-density polymer melt surfaces, which combines ideas from the traditional self-consistent field theory and the Sanchez–Lacombe equation of state theory [13–15], is the one developed by D.N. Theodorou [16,17]. Details of theoretical formulation will not repeated here as they can be found in the original work done by Theodorou [16,17].

The systems studied consisted of three phases: a solid surface *s*, an interfacial polymer phase *f* and bulk polymer *b*. According to the assumptions of this variable-density model [16]:

1. The solid surfaces are molecularly smooth, energetically homogeneous and impenetrable by polymers. They extend in the *x*- and *y*-directions infinitely, and end effects are neglected.
2. In phases *f* and *b*, the polymer is represented as a simple cubic lattice, whose sites are filled by chain segments and voids. The bulk polymer phase is infinite in extent. The density of the polymer phase can be adjusted to changes in temperature and pressure, as well as to the special energetic and entropic conditions prevailing at the interface, through changes in the local concentration of voids.
3. The Bragg–Williams approximation of random mixing is used to account for excluded volume effects in a layer-wise fashion. A layer-wise mean-field approximation is also used in calculating the energy of segment-segment interactions and intramolecular energy.

Three parameters describe the nature of the fluid. These are the chain length *r*, the attractive energy between adjacent segments w_{AA}, and the segmental volume v^*.

The volume of the polymer segment inside the lattice site is calculated using the Flory segment. The Flory segment, of length l_F, is usually shorter than the Kuhn segment. It can be defined such that a chain will have the same maximally extended length (end-to-end distance in all-trans conformation) and volume as they are measured experimentally. On the other hand the length of Kuhn segment (l_K) is related to stiffness parameter C_∞ by the expression, $l_K = l_b(C_\infty/\sin(\theta_b/2))$. The mean square end-to-end distance of the chain is $\langle R^2\rangle = C_\infty n_b l_b^2$, where l_b is the bond length and θ_b is the bond angle along the chain backbone and n_b is the number of bonds.

The Flory segment is calculated by the equation:

$$l_F = \left[\frac{n_m M_m}{N_A \rho n_b l_b \sin(\frac{\theta_b}{2})}\right]^{1/2}, \tag{1}$$

where n_m is the degree of polymerization, M_m is the monomer molecular weight, ρ the mass density of the polymer and N_A is Avogadro's number, n_b is the number of chemical bonds per chain.

The l_F (and the segmental volume) is initially calculated at an arbitrary temperature and determines the lattice site size and the number of Flory segments. As the temperature (or density) varies the changes in segmental volume are taken into account by the increase or reduction of voids volume fraction according to the Sanchez–Lacombe equation of state.

We also introduce, according to Sanchez–Lacombe theory, new parameters T^*, P^*, which are equivalent to the attractive energy between adjacent segments w_{AA}, and the segmental volume v^*:

$$T^* = -\tilde{z}\frac{w_{AA}}{2k}, \tag{2}$$

$$P^* = \frac{RT^*}{v^*}, \tag{3}$$

and

$$T_s^* = -\frac{w_{AS}}{k}, \tag{4}$$

where *k* is Boltzmann's factor, *R* is the ideal gas constant and $\tilde{z}$ is the coordination number (for example for cubic lattice, $\tilde{z} = 6$).

From these new parameters we define the corresponding Flory–Huggins parameters:

$$\chi = \frac{T^*}{T}, \tag{5}$$

for the virtual interaction between polymer segments and voids

$$\chi_s = -\frac{\tilde{z}T_s^* - T^*}{T}, \tag{6}$$

for the interaction between polymer segments and surface. The last parameter takes negative values when describing adsorption. In order, our theoretical results, to be easier compared with experimental we mention that in experiment is also used the following parameter, $\chi_s' = \lambda_1((\tilde{z}T_s^* - T^*)/T)$, which takes positive values for the case of adsorption, λ_1 is the fraction of the sites lying in adjacent layers (for cubic lattice it is 1/6).

For a given temperature *T* and pressure P_b in the bulk phase, the volume fraction of chain segments in bulk, ϕ_b, is calculated by equation:

$$\frac{P_b v^*}{RT} + \left(1 - \frac{1}{r}\right)\phi_b + \ln(1-\phi_b) + \chi\phi_b^2 = 0 \tag{7}$$

The rest formulation is similar with previous works [6,18–27].

We have also used the block version [28] of the nSCF method mainly in order to obtain orientation characteristics and developed forces when polymeric systems approach each other. In this method the blocks (Scheme 1(a)) of mixtures contain several polymer segment, filling the entire block with polymer. In case of solution it contains solvent molecules too. Also an empty lattice site (voids) is introduced in accordance with traditional nSCF [16,17]. In this way polymer density fluctuations are described by the concentration of voids.

The possible segment conformations inside a cubic block are shown in Scheme 1(a). Each conformer is characterized by the side of the cube on which the ends of the segment are put. As this is a one-dimensional model characterized by the *z*-component, the *x*- and *y*-axes are equivalent. Hence conformers are in general degenerate. In our model the conformer sc = 1 is not degenerate, the conformer sc = 2, sc = 5, sc = 6 and sc = 7 has a two-fold degeneracy and the conformers sc = 3 and sc = 4 have a four-fold degeneracy (see Ref. [26]). In these models the segment conformations and so the total polymer conformation are not restricted by the lattice. We mention that the lattice size (l) is equal to l_F in the nSCF model [26] and equal to l_K in the bnSCF model [28].

In melt the adhesion tension is calculated by the following equation [16,28]:

$$\frac{2(\gamma-\gamma_s)a_s}{kT} = m\left(\frac{P_b v^*}{RT}\right) + \sum_{i=1}^{m}\left[\left(1-\frac{1}{\bar{r}}\right)\phi_i + \ln(1-\phi_i) + \chi\phi_i\langle\phi_i\rangle\right], \tag{8}$$

where a_s is the area per site, *m* the number of layers, $\bar{r}$ is the average chain size, $\gamma - \gamma_s$ the surface tension at polymer/solid interface. The volume fraction of polymer (in the "solution" of voids) is ϕ_i. The average $\langle\phi_i\rangle$ is defined in terms of the volume fractions of adjacent layers, as $\langle\phi_i\rangle \equiv \langle\phi_i(z)\rangle \equiv \lambda_1\phi_i(z-1) + \lambda_0\phi_i(z) + \lambda_1\phi_i(z+1)$.

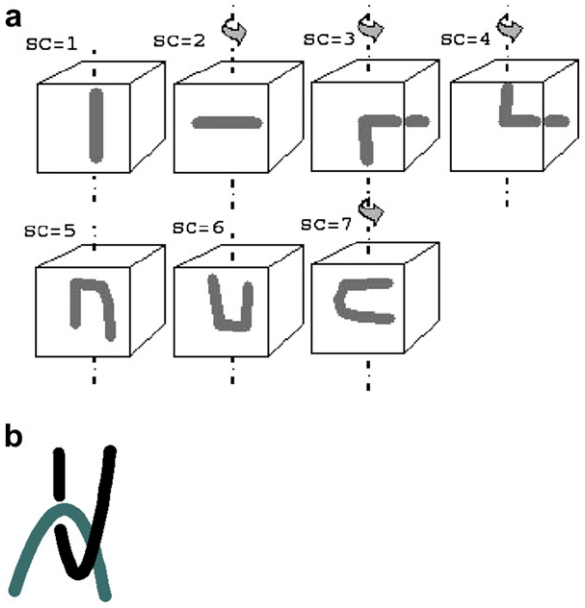

Scheme 1. (a) The seven possible polymer-segment conformations (*sc*) inside the cube lattice site for the bnSCF method [28]. In melt case the block (lattice site) is filled with polymer. (b) The coexistence of the 5th (sc_5) and 6th (sc_6) conformations is considered as a measure of entanglement in vertical direction.

The force per plate area ($\widehat{a}$) is:

$$\frac{F}{\widehat{a}} = -2\frac{\mathrm{d}}{\mathrm{d}D}[\gamma - \gamma_c], D \ll \widehat{a}^{1/2}, \tag{9}$$

where D is the distance between the plates.

In order to study the mechanical properties of the polymer–surface interface, we apply an algorithm for generating polymer entanglement network [29]. The network is created using as guides the configurational distribution functions derived from the SCF data in the interfacial region. The entanglement points are placed equidistant along each macromolecular chain of the network, but simultaneously they follow the statistical weights of the SCF theory (in the direction perpendicular to the surface). The initial position of the entanglement points of each chain parallel to the interface obeys Gaussian random walk statistics. The present procedure creates a macromolecular network which is not in equilibrium. The relaxation of this network is achieved by Monte Carlo methods involving moves that preserve the placement of entanglement points in the directions perpendicular to the interface. The relaxed polymeric network is our starting point for the study of the fracture phenomena, caused by the application of tensile stress perpendicular to the interface. The networks created by this procedure are not mechanically relaxed. In order to achieve a more uniform density, we then apply a method for relaxing the network with respect to its density distribution. The condition of mechanical equilibrium is imposed by minimizing the free energy functional of the macromolecular network. Contributions to the free energy include (a) the elastic energy due to stretching of the chain strands, and (b) the free energy due to the repulsive and attractive (cohesive) interactions between segments. In order to calculate the interaction energy, a simple cubic grid is superimposed on the network. The repulsive interactions are calculated within each grid cell. The attractive interactions are calculated from contributions between cells and within each cell. The fully relaxed networks serve as a starting point for the mesoscopic simulation of fracture phenomena, caused by the application of tensile stress perpendicular to the interface. The network is deformed at a constant strain rate and the network topology evolves according to elementary mechanical processes of chain scission, chain slippage, disentanglement, and re-entanglement. Chain slippage across an entanglement point occurs according to a Zhurkov activated rate

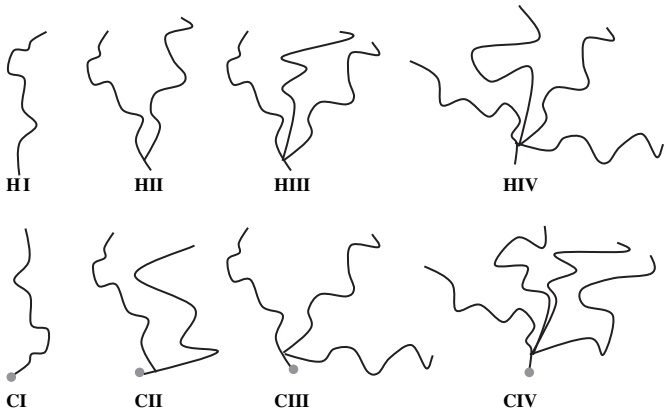

Scheme 2. Schematic representation of the polymer architectures used in our study. All structures are mainly based on propylene monomers. The homopolymers are names as HI, HII, etc. depending on the number of branches (H stands for the homopolymer and I, II, etc. for the number of branches). Polymers functionalized at one end by an ionic group are names as CI, CII, etc. depending on the number of branches (C stands for the copolymer and I, II, etc. for the number of branches).

Table 1
Macromolecular chain species investigated in the present article. PP copolymer chain is a PP chain with an end group at one end of the chain. Star (branched) polymers have a short central piece (two Flory segments long). In the copolymer samples the end group is attached at the end of the short arm. In the second column we specify the average molecular weight (in Flory segments) of the polymer studied. In the third and fourth column, it is specified the figure and the table respectively, in which results for the respective macromolecule appear. All samples are monodisperse except the linear PP homopolymer with average size of 100 segments, which shows various PDIs from 1.02 (practically monodisperse) to a maximum value of 2.

Type of polymer	Average chain size (in Flory segments)	Figure	Table
HI (PP homopolymer, linear)	100	2, S3, 6, 7	3
	156	1, 2	
	256	S1, S2, 2, 3, 4	2
	510	1, 2	
	764	1, 2	
	1016	2, 5	
HII (PP homopolymer, two branches)	510	S1, S2, 2	2
HIII (PP homopolymer, three branches)	764	S1, S2, 2, 3, 4	2
HIV (PP homopolymer, four branches)	1018	2, 5	
CI (PP copolymer, linear)		8, 9	4
CII (PP copolymer, two branches)		8	4
CIII (PP copolymer, three branches)		8, 9	4

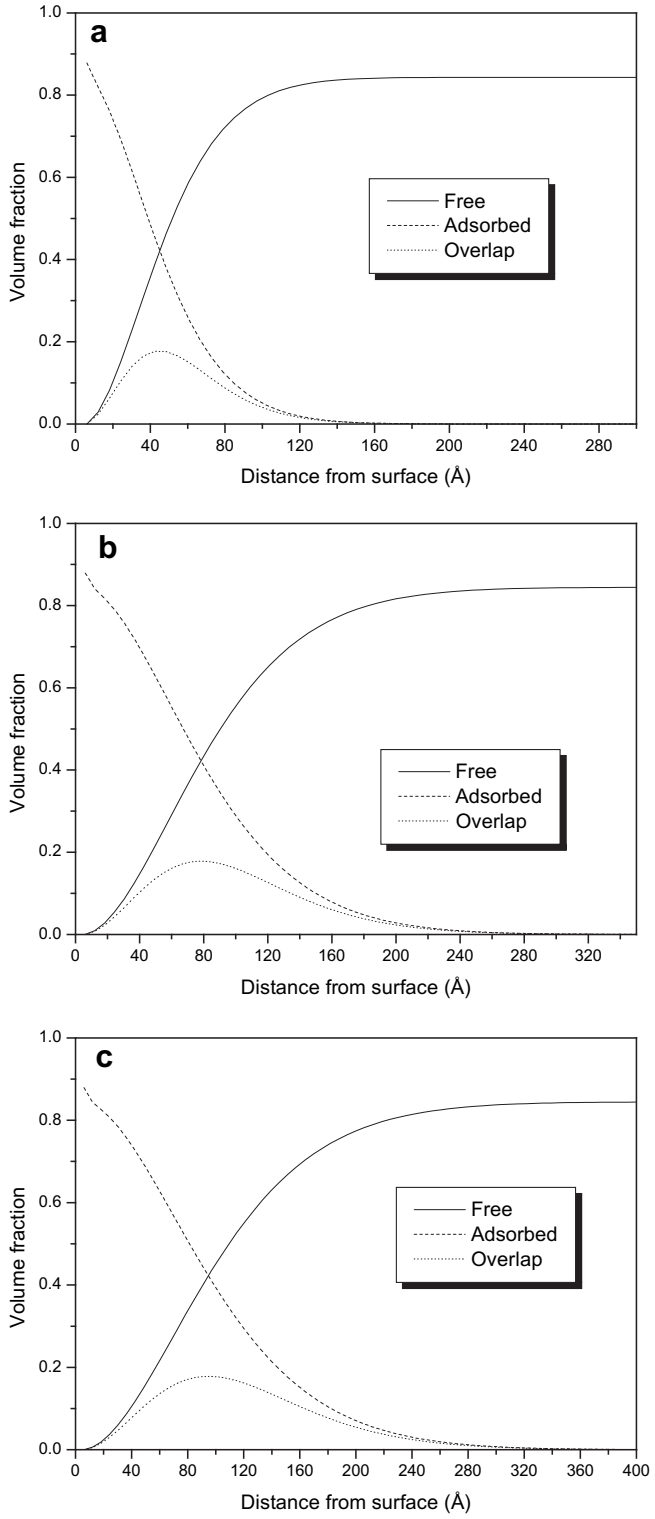

Fig. 1. Volume fraction profiles of adsorbed (dashed curve), free (solid curve) PP linear chains (HI-type) and product of free and adsorbed volume fraction (dotted curve) as a function of the distance from the surface. The parameters of the system are: $P = 1$ bar, $T = 493$ K, $T^* = 700$ K and $T_s^* = 400$ K. The chain size in Flory segments (one Flory segment contains 2.37 monomers) is (a) 156, (b) 510 and (c) 764. The integral of the overlap region (product of free and adsorbed, dotted curve) is (a) 10.95 Å, (b) 19.93 Å and (c) 24.35 Å.

equation with parameters derived from viscosity data. Each cycle of the kinetic MC algorithm used to track the deformation process consists of the imposition of a small incremental strain on the

Table 2
Structural characteristics of the product curve of free and adsorbed chains, for monodispersed PP homopolymers plotted in Fig. S2.

	Integral	Width	Position of maximum
HI	14.07 Å	181.80 Å	54.53 Å
HII	19.77 Å	254.52 Å	78.78 Å
HIII	21.81 Å	272.70 Å	90.89 Å

network, relaxation to mechanical equilibrium, introduction of the micromechanical processes mentioned above, and again relaxation to mechanical equilibrium. The MC cycles are repeated until fracture occurs [29,30]. The method is exactly the same one with the one applied in our previous publications [29,30], with the only exception that we introduce an interaction energy for the adsorbed polymer segments. This energy is representative of the Flory–Huggins interaction parameter used to describe in a mean-field way the interaction between polymer segments and surface. Hence we have introduced two new microscopic deformation processes. One is the creation of a weak van der Waals bond once an entanglement or an end point come very close to the surface and the other is the breaking of this weak bond. The creation of the bond occurs once an end segment or an entanglement gets a position, which is shorter than half of one Flory segment. The new position of this segment is on the surface ($z = 0$) keeping the same x- and y-coordinates. Obviously, the entanglement segments that are now 'chemically' bonded to the surface do not contribute to the slippage and disentanglement micro-mechanisms. The other microscopic deformation process, describes a breaking of this bond following a 'Zhurkov-type' activated rate expression depending on the local stress situation around the point on the surface [29,31]. The expression for the rate constant of an elementary breaking of the new bonds event is given by the expression,

$$k_{\text{breakdW}} = k_0 \exp\left[-\frac{E^* - l_K F}{kT}\right]. \tag{10}$$

The activation energy is estimated from representative end group-surface interaction energies. Here we assume zwitterionic

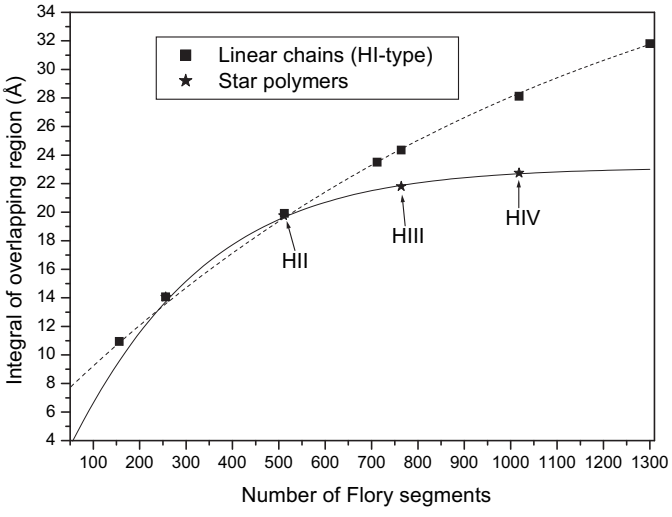

Fig. 2. Integral of overlapping region as a function of average chain size (in Flory segments). Data for the linear chains are depicted by square symbols and data for the branched polymers are plotted by star symbols. The theoretical predictions for both species have been fitted by a 'Sigmoidal-Boltzmann' function, plotted by solid curve for the star polymers and dotted curve for the linear chains. The function that describes the fitting is of the form: $f(x) = [(-368.532/(1 + e^{(x+2321.6)/1054.3})) + 43.242]$ (macromolecules of linear architecture), $f(x) = [(-96.985/(1 + e^{(x+298.89)/244.27})) + 23.136]$ (star-polymer architecture).

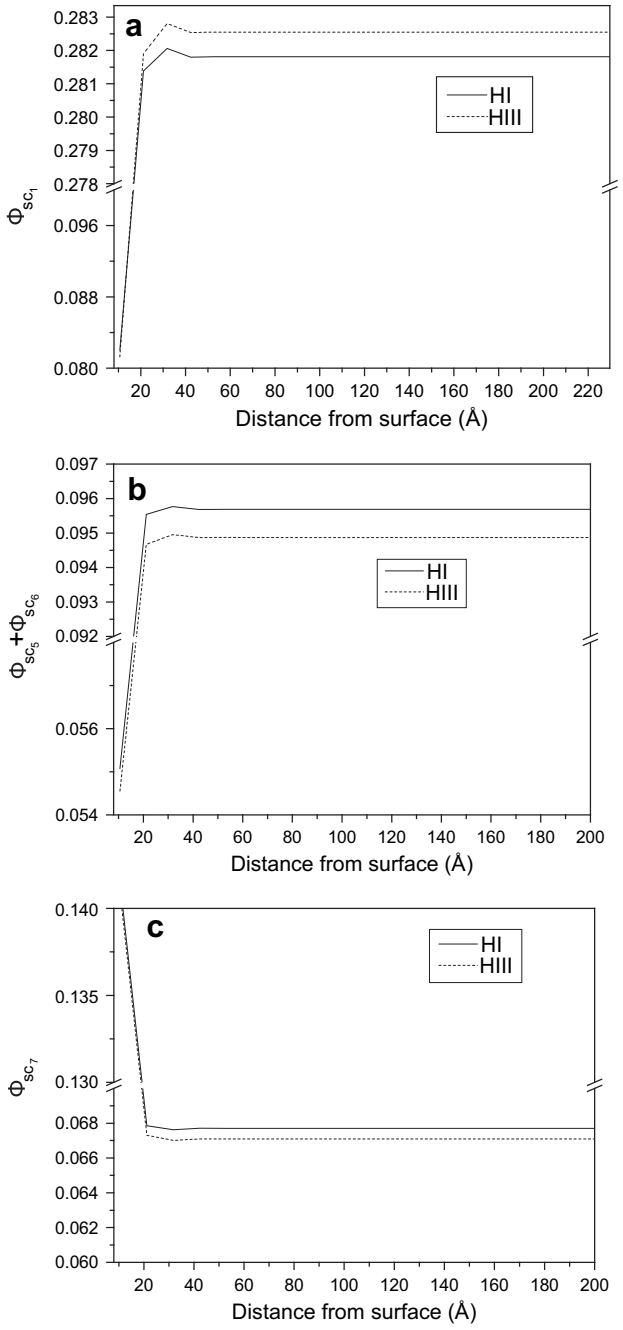

Fig. 3. Plots of volume fraction profiles of various segment conformations. (a) Volume fraction of segment conformation sc_1 as a function of the distance from the surface, which is a measure of chain vertical to the surface orientation. (b) Summation of volume fractions of conformations sc_5 and sc_6 as a function of the distance from the surface, which is a measure of chain vertical to the surface orientation. Conformations of this kind enrich the sample with entanglements of type shown in Scheme 1(b). We mention that on the surface the volume fraction of sc_5 is zero. (c) Volume fraction of segment conformation sc_7 as a function of the distance from the surface, which is a measure of chain parallel to the surface orientation.

end groups and we use a value of 7–8 k_BT (see Ref. [28]). This corresponds to activation energy of 4.74 kcal/mol (compare to 11.2 kcal/mol, the activation energy used for the chain slippage process, see Ref. [29]). F is the force estimated on the segment bonded on the surface due to the strand connected to it. For the frequency factor k_0, we use the same value used in the other processes (Ref. [29]), in order to avoid introducing several new parameters.

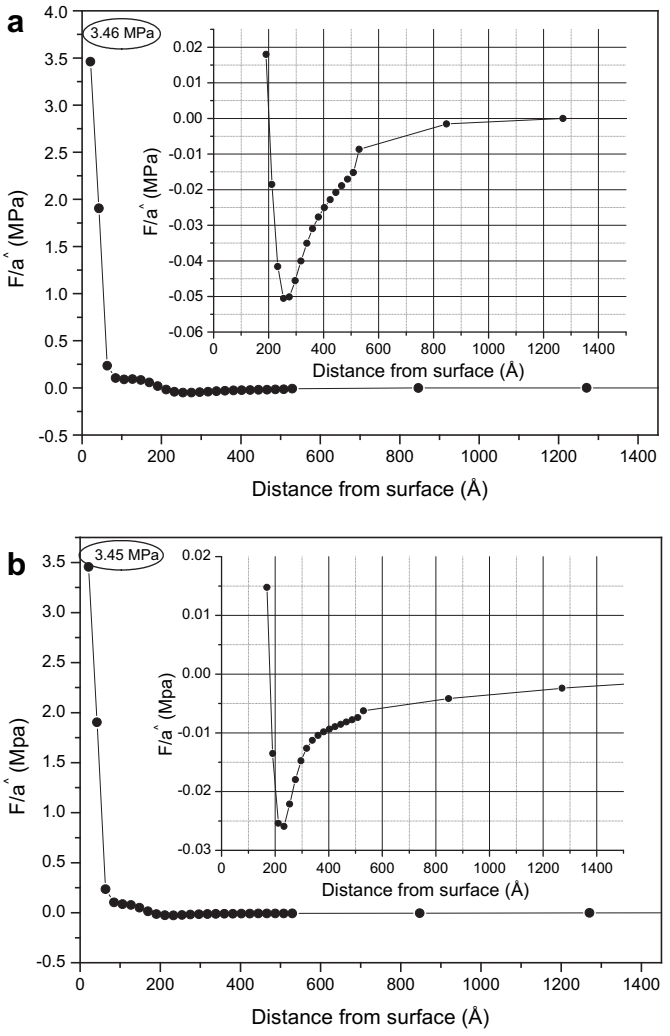

Fig. 4. Plots of the forces per plate area $\hat{a}$, estimated from Eq. (9). Negative values describe attraction while positive repulsion. (a) HI-type linear PP polymer and (b) HIII-type PP polymer.

3. Model system

In the present study we have investigated isotactic polypropylene (PP). The statistical mechanical properties of the PP polymer under investigation correspond to melt phase (i.e. a temperature at 493 K). Although commonly usage of PP is found at a temperature below melting point (459 K [32]), the chains conformations of higher temperature are usually preserved at these lower temperatures as the samples are prepared by fast cooling of the high temperature (well above the melting point [24,26]) PP polymer.

We have investigated homopolymers and copolymers in order to obtain information about their behavior. They can have linear or star-polymer architecture. The polymers investigated are named after their type and the number of their branches. Hence the PP homopolymers labelled by the symbol H and the copolymers by the symbol C. Then, the linear homopolymer chains are labelled as HI and the star homopolymers as HII, HIII and HIV, with two, three and four branches respectively (see Scheme 2). The copolymers are linear or branched polymers with an end group present in the macromolecular chain [28]. Then, the copolymer chains are labelled as CI, CII and CIII, for macromolecular chains with one (linear chain), two, three and four branches respectively (see Scheme 2).

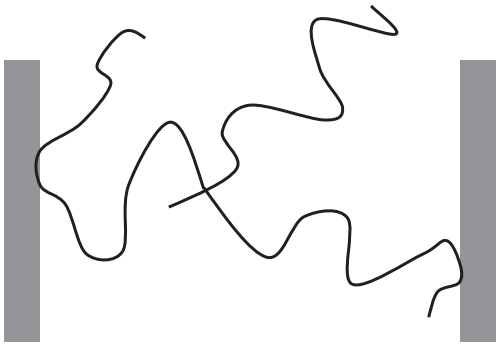

Scheme 3. Schematic presentation of an HIII star architecture adsorbed on both plates.

In the present study, the linear homopolymers, named as HI, have various molecular weights ranging from 15.528 kg/mol to 129.402 kg/mol, which corresponds to 156–1300 Flory segments. The homopolymers with star architecture (HII to HIV) have a short central part consisting of 2 Flory segments and branches of size equal to 254 Flory segments (25.283 kg/mol) each. The architectures and the molecular weights studied in the case of copolymers (i.e. PP chains with the presence of an end group with adsorbing capability) are the same as the one investigated in the homopolymer case. Now the major difference is that the adsorption is accomplished by the short (one Flory segment size) functional end group [28].

For $T = 300$ K, $P = 1$ bar and $T^* = 700$ K the calculated density by the equation of state (Eq. (7)) (far from surface) is 0.71 g/cm^3 while for $T = 493$ K is 0.63 g/cm^3. The present value for the parameter $T^*(= 700$ K) was chosen arbitrary in order to be close to parameters used in previous investigations (see Table II in Ref. [15]) of other polymers with similar characteristics. The characteristic ratio (C_∞) takes a value 5.7 [24,32]. For PP, the Flory segment length from Eq. (1) is $l_F = 6.06$ Å, and the number of chemical (propylene) monomers in a Flory segment is 2.37. In the block version of SCF model (bnSCF) [28] each block contains 1.75 Flory segments resulting in a lattice with layer (10.58 Å) 1.75 times larger than the one used in the nSCF methodology. In the rest of the work, when we are referring to segments we mean Flory segments. In the copolymer systems the Flory interaction parameters are χ_S (PP) = 1.42 and χ_S (end group) = −10.75.

The basic characteristics of the polymers investigated in this article are reported in Table 1.

4. Results and discussion

We start our investigations with the homopolymer PP case. First of all we have tried to determine the adsorption capability of a surface in order to adsorb linear (HI) and star polymer of architectures, HII and HIII equally well (Fig. S1, in the Supplementary data Appendix). We have found that for a representative linear HI chain with 256 Flory segments, the most appropriate value for the parameter T_s^* of Sanchez–Lacombe model is 400 K. The corresponding Flory–Huggins, χ_S, has the value −3.45. In our study we have found that this is the desirable value of surface Flory parameter, χ_S, which adsorbs with the same ability independently of the number of branches of the PP chain.

One of the major aims of our research is the detection of the optimum architecture of homopolymer PP chains that would increase the region of overlap between adsorbed by solid surface polymers and free (no adsorbed) polymer. As this overlap region is a rough estimate of the adsorption strength of the PP polymer melt with the surface.

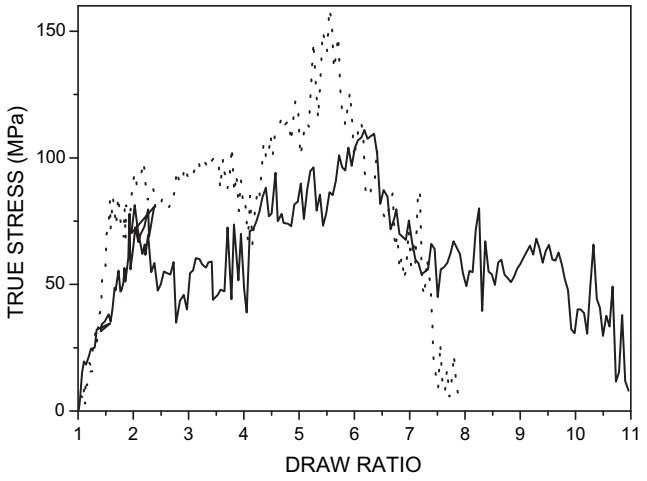

Fig. 5. True stress–draw ratio curves for linear PP samples with linear architecture (HI) and HIV architecture. The molecular weights are very similar as the linear polymer has 1016 Flory segments and the branched has 1018 Flory segments. The linear polymer is depicted by dotted curve and the HIV by solid curve. The deformation occurs at strain rate 1% per second.

4.1. Monodisperse homopolymer PP samples

We start our investigation with monodisperse samples of linear architecture. In Fig. 1, we plot the volume fraction profiles of the free chains, the adsorbed chains and the product of the volume fraction of the free and adsorbed chains. The latter is an estimate of the overlap region between the free and adsorbed macromolecules. As it is expected for linear macromolecules we observe (Fig. 1) that as the molecular weight increases the overlapping region between the free and the adsorbed chains increases. Actually, the relation between the areas of the overlap region (integral of dotted curve) with the molecular weight is almost linear for these low molecular weights (not shown). In accordance to what is expected from the overlap region information (Fig. 1), we have found that when we apply a tensile stress till the breaking of the sample, the shorter sample (Fig. 1(a)) is the easiest to fracture and the longest one (Fig. 1(c)) the hardest one. It is found that for these samples the strain at which the sample practically breaks is proportional to the area of the overlapping region (not shown).

Next in Fig. S2 (in the Supplementary data Appendix) we show how the overlap region varies with architecture. It is observed that as the number of branches increase the region of coexistence between adsorbed and free polymer (Fig. S2(a)–(c)) becomes wider. The overlap area, the width of the overlapping region and the distance from the surface of the overlapping region are reported in Table 2. In order to have a reasonable comparison between the branched and the linear chains, we concentrate on chains of different architecture but with almost identical molecular weight (Fig. 1(b), S2(b) and Fig. 1(c), S2(c)). It is found, as expected, that the longer linear chains exhibit a wider overlapping region comparing with polymers of star architecture of almost the same molecular weight. However it is important to point out that HIII star polymers with each branch having molecular weight 1/3 of the molecular weight of the linear macromolecule (Fig. 1(c), S2(c)), exhibit an overlapping region between free and adsorbed chains, comparable with the one found in the linear chains. This is a clear indication that linear branches of such star architectures (HIII) do not feel the same extension (brush effect) on the same adsorbing surface compared to the case where these branches would be adsorbed as separated (not-connected by the short central part) linear polymers (HI). An analogue conclusion for free

Table 3
Structural characteristics of the product curve of free and adsorbed chains, for polydispersed PP copolymers plotted in Fig. S4.

PDI	Integral	Width	Position of maximum
1.02	8.91 Å	115.14 Å	36.35 Å
1.05	9.09 Å	121.20 Å	36.35 Å
1.10	9.38 Å	127.26 Å	36.36 Å
1.20	9.93 Å	133.94 Å	36.36 Å
1.50	11.43 Å	163.61 Å	42.41 Å
2.00	13.51 Å	193.92 Å	42.42 Å

star polymers in melt was given by Daoud et al. [33]. The difference in the overlapping region between cases of polymers with linear and star architecture with the same molecular weight becomes more pronounced for greater molecular weights as shown in Fig. 2. The key feature toward the understanding of this behavior is the adsorption on the surface. Linear chains adsorption exhibits an almost linear increase at low molecular weights, although after some characteristic value they show reduction of the adsorption (not shown [34]). On the other hand it is known that star polymers with such architecture (although adsorbed to the surface in a different way) depict rapid reduction of the adsorption amount by increasing the number of branches due to entropic reasons [28]. Even though the 254 segment branch could possibly be stretched even further, closer to the all-trans conformation (depending on the adsorption strength), we realize that after a certain number of star chains have adsorbed on the surface (with respect to the number of branches), the brush cannot be stretched any more and 'make' space for other chains. In this case the rest area on the surface is covered by the already adsorbed chains. It is obvious that some branches are more stretched perpendicular to the surface than the linear case, while others take conformations more parallel (like a bunch of flowers) to the surface covering the whole region close to the surface [28]. It seems that for both cases (linear and star chains) the dependence of the overlap region on the molecular weight, at least for the region investigated (16–130 kg/mol), can be fitted well by a 'Sigmoidal-Boltzmann' function of the form $f(x) = ((A_1 - A_2)/(1 + e^{(x-x_0)/d_x})) + A_2$, where A_1, A_2, x_0, d_x are parameters (Fig. 2). The most important parameters in the functional form of $f(x)$, is A_2-parameter which indicates the asymptotic value that takes the overlapping integral and d_x-parameter which indicates how fast the asymptotic plateau value is reached (the smaller the faster). From Fig. 2, we conclude that the branched chains reach the asymptotic value much faster. Moreover, the plateau value of the linear chains is almost twice the one found in branched chains (Fig. 2). This is a clear indication that linear chains compared to highly branched chains of equal molecular weight have in general better adhesive properties.

An important structural property that can give specific information about the stretching of the chains close to the surface is the orientation of the chain segments perpendicular to the surface. For this reason we have studied the percentage of each block conformation, which also give us information about the kind of the formed entanglements. First, we point out that a significant increase of volume fraction of blocks that describe chain segments at a direction parallel to the surface (see Scheme 1(a)) is found, as expected, for distances close to the adsorbing surface (not shown). In Fig. 3(a) we plot the representative profile of the volume fraction of sc_1 conformer ($\phi_{sc_1}(z)$), which obviously depends on the polymer architecture, describing the total chain elongation perpendicular to the surface. The vertical orientation amount, for all H-type chains shows that segment conformations that do not 'feel' the presence of the surface are reached soon, almost from the 4th layer of the lattice. Moreover, we see that the HIII chains show larger alignment along the vertical direction comparing to the linear chains. This

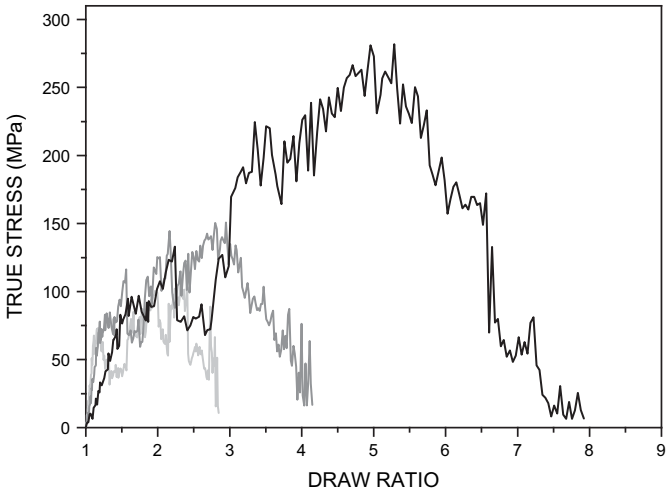

Fig. 6. True stress–draw ratio curves for linear PP samples with Schultz–Zimm Distribution. The samples correspond to the cases (a), (e) and (f) of Fig. S3. The deformation occurs at strain rate 1% per second. Light gray curve for PDI = 1.02, dark gray curve for PDI = 1.5 and black curve for PDI = 2.0. In addition, we can distinguish the various samples by the fact that the fracture occurs at increasing draw ratio with increasing PDI index.

finding is in accordance with the results of volume fractions of the free and adsorbed chains (Fig. S2). Another indication of the vertical alignment of the macromolecular chains is reported by means of the Fig. 3(b). In this plot we report the volume fraction profiles of conformations sc_5 and sc_6 (both conformers with vertical orientation with respect to the surface, see Scheme 1(b)), which is a measure of the sample orientation along direction vertical to the surface. Now, we observe that in HIII star polymers the volume fractions are reduced compare to liner polymers (Fig. 3(b)). This is an indication of the fact that the sc_1 conformers contribute more in the orientation of the branched chains than the sc_5 and sc_6 conformers. On the contrary, as it is expected, the orientation of the chains in direction parallel to the surface, indicated by different type of conformers (for example sc_7 conformers, see Scheme 1(a)), shows exactly the opposite trend (Fig. 3(c)). The volume fractions of the sc_5 and sc_6 conformers can be used to get information related to the entanglements in the overlapping region. In Fig. S3 (Appendix), we plot the volume fraction of the sc_6 conformers of the free chains and the sc_5 conformers of the adsorbed chains. We find that the overlapping region, which is an indication of entanglements between free and adsorbed chains, is larger for the HIII polymer than the one for the HI linear polymer. This observation is in accordance with the findings of Fig. 1((a) and (c)) and Fig. 2 as it follows the trend of the total overlapping region.

Next, in Fig. 4 we study the forces per area that are applied when two identical surfaces (plates) approach each other (Eq. (9)). This procedure is considered to be reversible (during stretching and compression there is no hysteresis in the free energy changes) in contrast to the stretching procedure which is calculated by MC deformation scheme. So the obtained pressure is expected to be lower comparing to the results obtained in the mechanical deformation study. We concentrate on two samples, linear (HI) and three-branch chains (HIII). According to the predictions of our method we have found, for both cases studied, that the forces very close to the surface are repulsive and have a value near 3.5 MPa. As the plates approach each other, brushes belonging to one plate feel the presence of the chains of the opposite plate and some chains may be adsorbed on both plates (see Scheme 3) and give higher adsorption and attractive forces (region 280–800 Å for the HI sample and region 230–1400 Å for the HIII sample in Fig. 4). To get

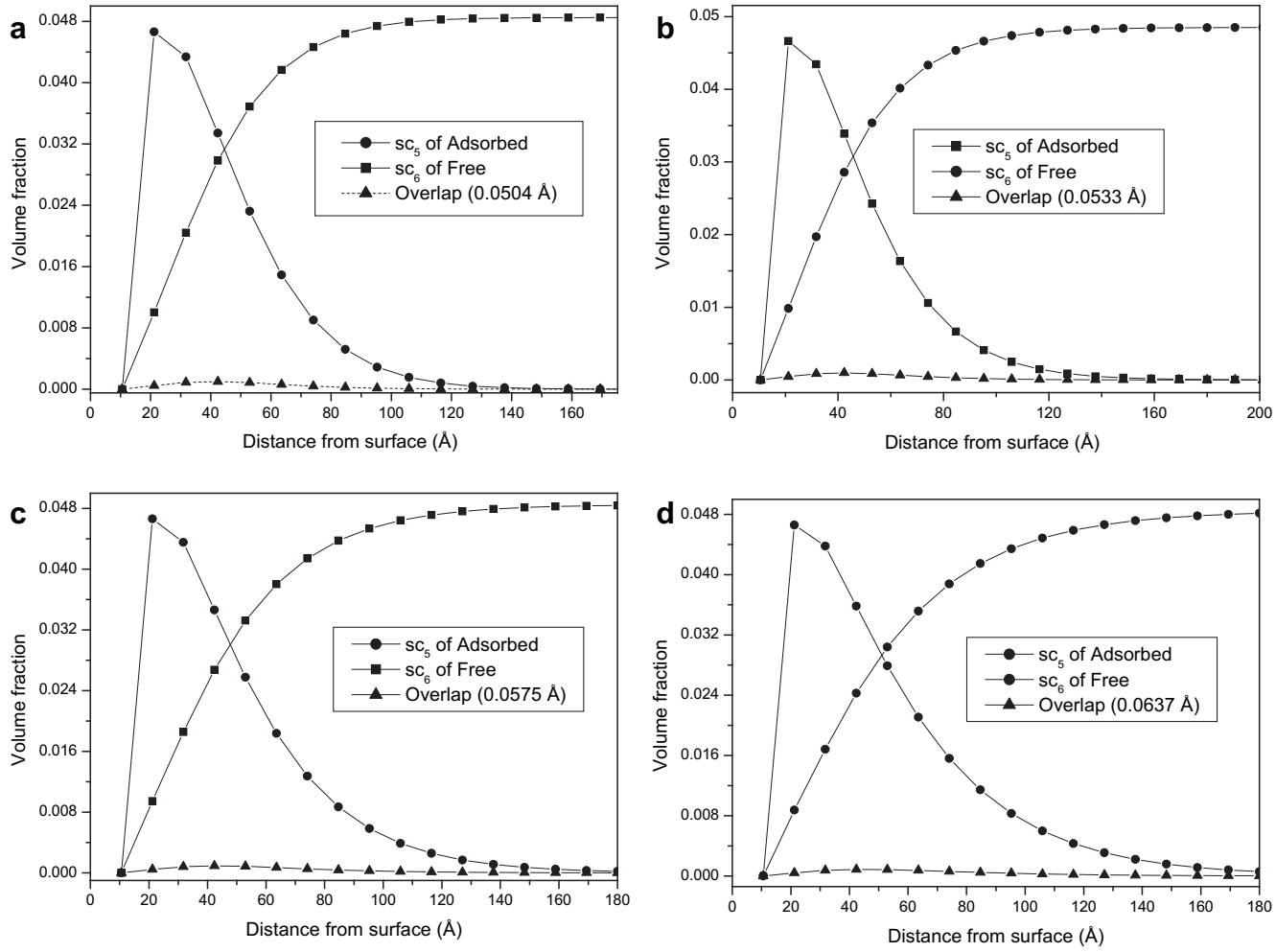

Fig. 7. Volume fraction profiles of sc_6 conformers of the free chains and sc_5 conformers of the adsorbed chains and the product of these volume fractions as a function of the distance from the surface. The overlap region gives an estimation of the entanglements that enhances stretching in the direction perpendicular to the surface (see Scheme 1). Molecular weight follows Schultz–Zimm distribution (Fig. S4). The polydispersity indexes are (a) PDI = 1.02, (b) PDI = 1.20, (c) PDI = 1.50 and (d) PDI = 2.00.

a better feeling of what is taking place in this process we mention that although the estimated from our models end-to-end distance for HI chain is around 100 Å, the all-trans conformation is almost 1550 Å long. Of course the statistical weight for conformations very similar to the all-trans conformation is very small and is reduced further with the increase of the intermediate distance between plates. That is mainly the reason to explain why the HI polymers start giving attractive forces at almost 800 Å. On the other hand, as already mentioned above, HIII polymers (i.e. star-shaped macromolecules) may be absorbed on both plates by different branches (Scheme 3). In this case the distance at which they can justify an attraction between the two plates even in a slow reversible process, is increased. After the end of this region (distances below 280 Å for HI and distances below 230 Å for HIII, see Fig. 4) due to entropic reasons the attractive force reduces. The first weak repulsion is observed at almost 190 Å for HI and 170 Å for HIII and is identified as the distance where the chains start to compress significantly and desorbs. It seems that HIII chains show slightly higher compressibility although stretched higher, probably due to the lower surface density (chains/adsorbing surface). Our findings suggest that some branches stretch significantly while the rest take parallel to surface conformations preventing other's macromolecules adsorption. Finally, we observe that the surface tension never becomes positive which means that there is no depletion.

We then investigate the fracture mechanics of two samples with the same molecular weight but different architecture. In Fig. 5 we depict the stress–strain curves of a linear sample containing 1016 Flory segments and a four branches sample (HIV) of 1018 Flory segments (four branches of 254 segments each and a 2 segments central piece). We have found that the linear sample is more difficult to break, as it is expected from the estimated overlap region (see Fig. 2). Actually, we have investigated other branched sample of similar molecular weights with the linear chains. We have found that the fracture occurs at comparable strains (not shown) in accordance to what is expected from the overlap region estimated in Fig. 2. We have found that it is the strain at break and not the area of the stress–strain (an estimate of the work done to break the sample) that correlates better with the overlap integral.

4.2. Polydisperse homopolymer PP samples

Then, we study the influence of the molecular weight distribution on the mechanical properties. We assume a Schulz–Zimm molecular weight distribution [24,35] with average size of linear chains equal to 100 segments and maximum size, which could be up to 1000 segments. For polymers of this molecular weights, the adsorption is accomplished with a lower value of polymer–surface interaction parameter, $T_s^* = 200$ K. This is the value used in the

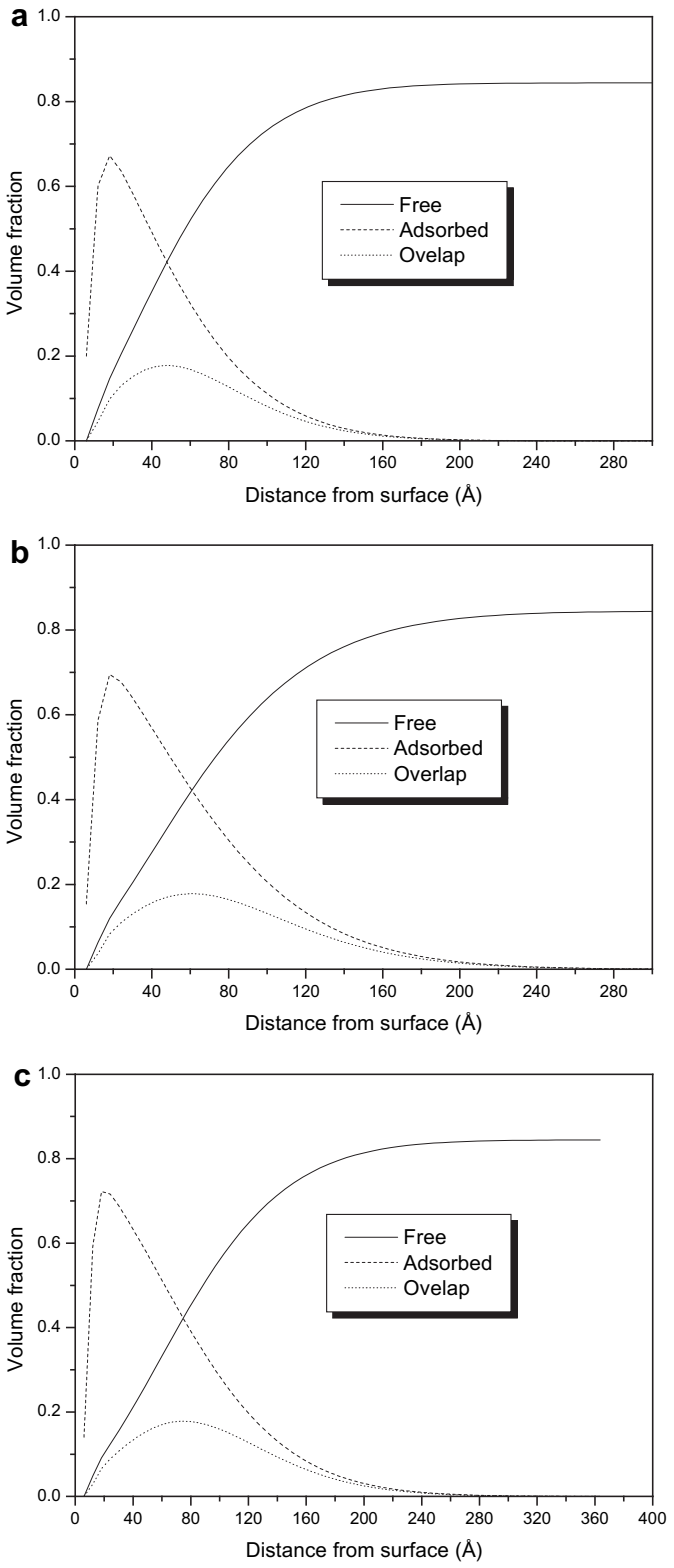

Fig. 8. Volume fraction profiles of C-types chains adsorbed by an end group on the short arm (similar with previous PS architectures [28]). $P = 1$ bar, $T = 493$ K, $T^* = 700$ K and T_s^* (end group) $= 1000$ K, T_s^* (PP) $= 0$ K. (a) CI with overlap region of 14.42 Å, (b) CII with overlap region of 19.42 Å and (c) CIII with overlap region of 21.81 Å.

study of the polydisperse samples, while all other parameters remain the same. The polydispersity index, PDI, takes values from 1.02 to 2. In Fig. S4 (Supplementary material), we plot the volume fraction profiles of the free chains the adsorbed chains and the product of the volume fraction profiles of the free and adsorbed chains. In Table 3 we report the integral of the product of the volume fraction profiles of the free and adsorbed chains, which is an estimate of the overlap integral and other important structural characteristics. We have found that the overlap region has a linear relation with the polydispersity index (the graph of the overlap integral versus the PDI is a line with slope ~4.69 Å, not shown). Although, the overlap region of chains seems to depend linearly on the polydispersity index, the mechanical properties show a rather different behavior. Actually, if we plot the draw ration at which fracture occur as a function of the PDI, the relation is highly non-linear. In Fig. 6, we show the two most extreme PDI value case of an almost monodisperse sample (PDI = 1.02), one with the highest (PDI = 2) and an intermediate one (PDI = 1.5). It is clearly observed the non-linear relationship between the draw ration at which fracture occur and the PDI. Actually, for the high polydispersity index system, even the first linear part is not the same as in the other two samples. We believe that the observed difference should be attributed to the extremely wide range of macromolecular chains existing in samples where molecular weight distribution shows Schulz–Zimm distribution. As the percentage of short chains (even 'chains' with one segment, i.e. monomers) is high, the demand of average chain size equal to 100 segments is fulfilled by the existence of few, very long chains which most probably make the sample behave very differently during mechanical deformation.

Table 4
Structural characteristics of the product curve of free and adsorbed chains, for monodispersed PP copolymers plotted in Fig. 8.

	Integral	Width	Position of maximum
CI	14.42 Å	181.80 Å	48.48 Å
CII	19.42 Å	242.40 Å	60.59 Å
CIII	21.81 Å	260.58 Å	72.71 Å

In order to check the validity of our arguments concerning the highly non-linear behavior of the mechanical properties in the Schulz–Zimm distribution, we have systematically investigated the orientational properties, by means of the volume fraction profiles of specific conformers. In our bnSCF method, an estimate of the entanglements that can contribute greatly for deformation of the PP sample in directions perpendicular to the surface is achieved from the segment conformations sc_6 of free (adsorbed) chains and the segment conformations sc_5 of adsorbed (free) chains (see Scheme 1(b)). In Fig. 7, we plot the volume fraction of the sc_6 conformers of the free chains and the sc_5 conformers of the adsorbed chains for most of the samples studied in Fig. S4 and in Table 3. We find that the overlapping region, which is an indication of entanglements between free and adsorbed chains, has a linear relationship with the PDI (intercept at 0.03701 Å and slope 0.01344 Å). This observation is not in accordance with the findings of Fig. 6, where there is no linear relation between the strain at which fracture or the integral of the stress–strain curve and the PDI. At this point we mention that the area below the stress–strain curve fits better with the overlap integral comparing to the fit of the strain at break with the overlap integral.

4.3. Copolymer samples

Next, we investigate linear and branched polymers with an end group present in the macromolecular chain [28]. Now we have copolymer PP samples as an end group with adsorbing capability substitutes the first segment of the short arm. These samples are named, as mentioned in the Model system section, as CI, CII and CIII depending on the number of branches. In this case where the chain adsorption is accomplished by an end group [28] the observed

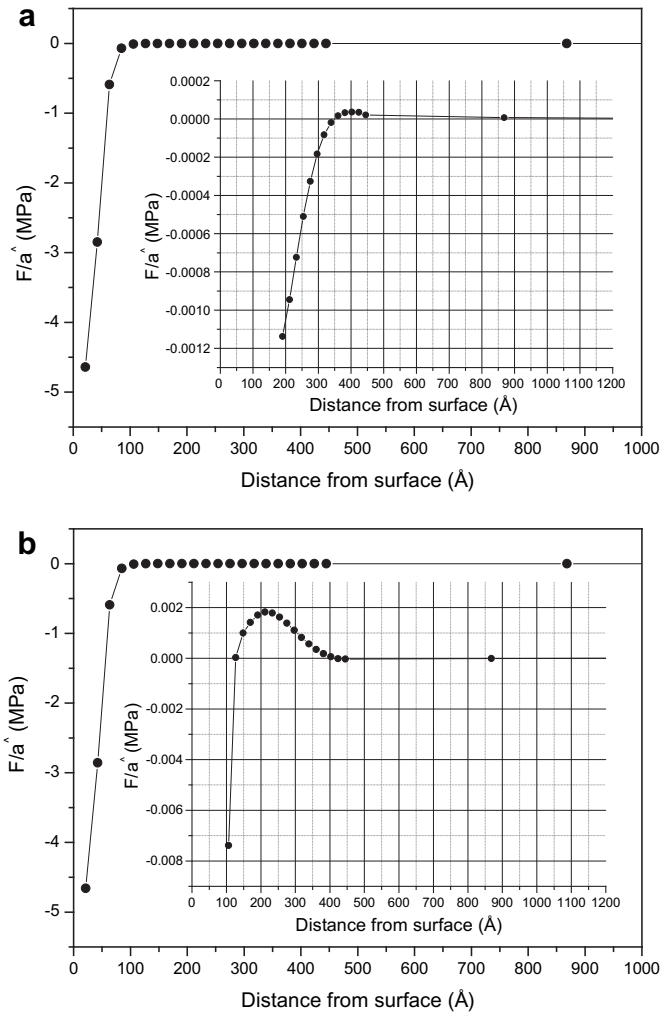

Fig. 9. Forces per plate area $\hat{a}$, for the two of the three cases studied in Fig. 8 types. (a) CI and (b) CIII.

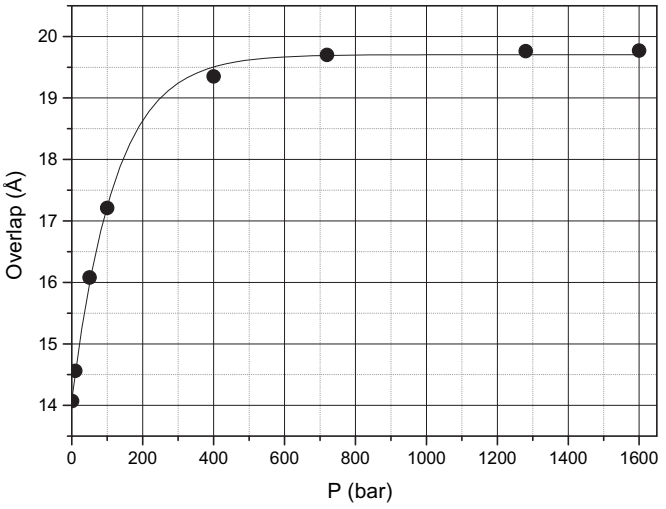

Fig. 10. Overlap integral versus external pressure for HI-type linear PP chain of 256 Flory segments. The predictions of the nSCF model are best fitted by the function: $f(x) = (-163.894/(1 + e^{(x+396.64)/118.74})) + 19.704$. The parameters of the system are: $T = 493$ K, $T^* = 700$ K, $T_s^* = 400$ K and $C_{inf} = 5.7$.

behavior is found to be quite different. Although the overlap region seems to follow the same (comparing to the homopolymer case) scaling with the increase of the number of branches, the density on the surface is dramatically decreased due to depletion of these chains (see Fig. 8 and Table 4). The interaction parameter between the end group and the surface is not an important parameter, as we do not compare to a realistic case. So we set the respective parameter equal to zero (i.e. $T_s^*(\mathrm{PP}) = 0$, see Fig. S1 for T_s^* value below 400 K). In addition, we have estimated the forces per plate area, obtained by the compression of two identical plates. In this copolymer case, we have found an attractive behavior in short distances (compare to homopolymer case, see Fig. 4), which can be attributed to the increase of polymer volume fraction on the surface for very short distances between plates (see Fig. 9). If we imagine the plates being very close, the chains of both sides although not adsorbed in opposite plate interlace with opposite macromolecules. If the distance between plates is increased an attractive force appears until the chains disentangle. It seems branched macromolecules disentangle faster. The increase in polymer volume fraction according to Eq. (8), justifies a more negative free energy (adsorption on the surface) which gives according to Eq. (9) attractive forces. We also observe that the distance at which the approaching brushes start to 'feel' each other is much shorter than the one found in the case where the polymers do not have an end group (see Fig. 4 for comparison). Now for both polymers investigated (i.e. CI linear polymer and CIII three branches polymer) the onset occurs at around 450 Å (Fig. 9). The basic reason has to do with the fact that in this case the chains cannot make bridges by adsorbing to both plates (Scheme 3). An almost full elongated chain but also adsorbed in both plates (homopolymer chains) loses substantially in statistical weight because of entropic reasons but has a small enthalpic gain due to adsorption. With the absence of this gain, in this case of polymers with end group, such conformations vanish and the significance of the extra stretching due to star architecture is reduced. After this characteristic distance the two plates repulse each other.

4.4. Effects of external pressure

Finally, we investigate the effects of the external pressure on the PP interfacial system for monodisperse homopolymer architecture samples (HI-type linear PP chains). For low values of the external pressure (in the range of few bars), increasing the pressure in the bulk polymer phase did not affect significantly the area of the overlap region (not shown). In this low-pressure regime, external pressure mainly influences density according to the equation of state while the width of the overlap is practically invariant. In Fig. 10, we plot the overlap region integral as a function of the external pressure. We find that for pressure up to a value close to 200 bar the overlap region integral and the pressure are almost proportional. But as we investigate samples with higher external pressure, the reported behavior becomes quite different. Actually, after some characteristic value of the pressure (obviously depending on the polymer sample, here we have investigated linear chains only) the overlap region is unchanged (plateau region in Fig. 10). The behavior observed in Fig. 10, can be explained by means of the volume compressibility, which is a basic polymer characteristic that is necessary for understanding polymer behavior under external pressure as it estimates the volume change under constant pressure. The behavior of the isothermic volume compressibility, for fixed temperature, is well-known (see for example Fig. 1 in Chapter 1 of Ref. [36], where the bulk compressibility decreases with increase of the pressure). Actually, the compressibility as a function of the temperature almost follows the trend depicted in Fig. 10. On the contrary, the fracture properties of the linear PP samples are rather unexpected. In Fig. 11 we plot the

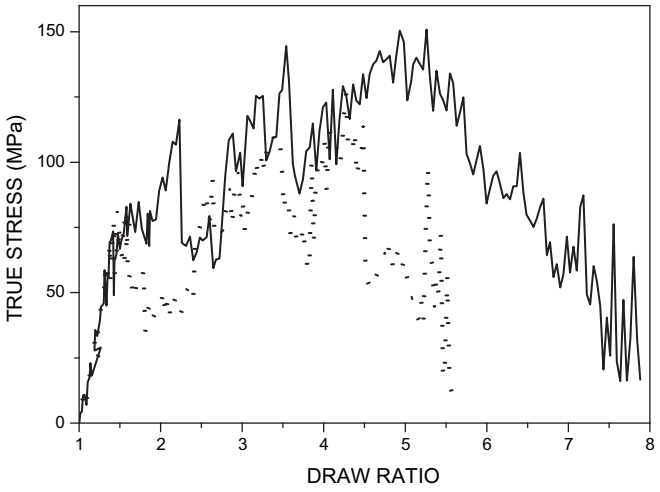

Fig. 11. True stress–draw ratio curves for HI-type linear PP chain of 256 Flory segments. The deformation occurs at strain rate 1% per second. The samples correspond to the cases of 720 bar and 1600 bar of Fig. 10.

stress–strain curve for two samples prepared under different external pressure (720 bar and 1600 bar, respectively), showing very similar overlap regions (see Fig. 10). We observe that the fracture mechanics properties are rather different despite the similarity in the overlap integral. This can only be explained once we realize that although the overlap region is the same, many other structural properties are quite different for samples prepared at different values of the external pressure. Actually, it is surprising to realize that the reported behavior for various high values of the external pressure is similar to recent experimental investigations [37]. Especially in the pressure regime of interest (Fig. 11), as the draw ratio increases, the polymer, which is already restricted to smaller space due to high pressure, is even more immobilized showing different fracture mechanisms (see Fig. 4 in Ref. [37]). Next we try to get a better understanding by means of the study of some orientational properties. In Fig. S5 (Appendix) we present the volume fraction profiles of the all-trans sc_1 conformers. We observe that as pressure increases the volume fraction of the all-trans sc_1 conformers increase. In other words as we increase the external pressure the part of the polymer that is tied on the surface and stretched due to entropic reasons takes more glassy conformations in the perpendicular to the surface direction. While the volume fraction of the other 'low mobility' conformations as the sc_2 conformation (i.e. parallel to surface conformers) is reduced (not shown). We believe that it is reasonable to assume that during the stretching process, in the region where the sample becomes thinner, the part of the polymer that is "tied" by entanglements would show analogous behavior. Of course in this situation conformations like sc_1 would have significantly greater percentage. We mention that according to our method far from the surface the pressure does not influence the percentage of each block conformation (Scheme 1(a)). At this point it is very important to point out that the mechanical properties have been studied started from samples prepared at unity draw ratio. This means that the effects of different external pressure have been taken into account, through the nSCF method, only for the initial configurations (i.e. before the stretching procedure starts). It is expected that the external pressure will influence the segmental dynamics of the deformed samples. The most proper way, not introduced in the present study, of treating this Kinetic MC procedure will be by introducing a local density dependent friction factor for the chain slippage procedure.

Before closing we remind the reader that polypropylene is a semicrystalline polymer. In the present investigation, as all statistical mechanical properties studied at a temperature above the melting point (and hence above the glass transition temperature), we need no take into account this fact. However, for our investigations in cases characterized by very high external pressure and in case of lower temperatures (for example room temperature), it is necessary to take into account the semicrystalline structure of PP. Actually, it is well-known that semicrystalline PP has significantly different mechanical properties compared to the amorphous PP, as it is expected due to different morphology and orientation close to the interface [38]. Our recently developed mean-field method (bnSCF [28]), can be easily adjusted so that treats properly semicrystalline polymers. This is achieved by properly re-weighting various conformations. The study of polymeric systems under external conditions such that the semicrystallinity is important, is one of our future projects.

5. Conclusions

In this article we have investigated polymeric systems under constant external pressure. The latter is achieved by means of a variable-density model. We adjusted an existing variable-density model, based on the equation of state of Sanchez–Lacombe, in order to take into account stiffness. This is practically achieved by assigning different bending energies to different bending angles formed by triplets of segments. This is an extension of our recently developed numerical self-consistent mean-field method (block SCF approach). Our aim is to study mechanical properties of polydisperse PP polymer brushes of variable density in the interfacial region (i.e. region between solid surfaces and polymer melt). The block version of the nSCF method allows for a better insight investigation of the structural properties of the polymer as for example the overlapping region of adsorbed chains and free chains and the kind of entanglements present. Forces developed under compression of two similar samples and stress–strain curves are also estimated revealing the mechanical behavior of the macromolecular system. We have found that the mechanical properties are strongly depend on the molecular architecture (linear/star chains), on the molecular weight and the molecular weight distribution. Finally, the mechanical properties have a dependence on the external pressure. In many cases studied the observed behavior on the fracture mechanics is in accordance to estimates from the structural properties of the interfacial macromolecules, except for the high-pressure cases.

In general the improved SCF numerical method is proved to be adequate for quantitatively reproduce the main features of the system under study. The future plans with these tools will include the systematic study of other more complicated architectures.

Acknowledgements

This work was supported by the Greek Secretariat for Research and Technology (GGET) by a grant (PENED 03ED856).

Appendix. Supplementary material

Supplementary data associated with this article can be found in the online version, at doi:10.1016/j.polymer.2009.09.030.

References

[1] DeGennes P-G. Scaling concepts in polymer physics. Cornell: Cornell University Press; 1979;
Eisenriegler E. Polymers near surfaces. Singapore: Word Scientific; 1993;
Granick S. Polymers in confined environments. Berlin: Springer; 1999;
Jones RAL, Richards RW. Polymers at surfaces and interfaces. Cambridge: Cambridge University Press; 1999.

[2] Cohen Stuart MA, Cosgrove T, Vincent B. Adv Colloid Interface Sci 1986;24:143;
DeGennes P-G. Adv Colloid Interface Sci 1987;27:1989;
Szleifer I. Curr Opin Colloid Interface Sci 1996;1:416;
Fleer GJ, Leermakers FAM. Curr Opin Colloid Interface Sci 1997;2:308;
Chakraborty AK, Golumbfskie AJ. Annu Rev Phys Chem 2001;52:537;
Netz RR, Andelman D. Phys Rep 2003;380:1.
[3] Alexander SJ. J Phys (Paris) 1976;38:977;
Harpelin A, Tirrell M, Lodge TP. Adv Polym Sci 1992;100:31;
Taunton HJ, Toprakcioglu C, Fetters LJ, Klein J. Nature 1988;332:712.
[4] Brazhnik PK, Freed KF. J Chem Phys 1994;101:9143.
[5] Sebastian KL, Sumithra K. Phys Rev E 1993;43:R32.
[6] Scheutjens JM, Fleer GJ. Macromolecules 1985;18:1882.
[7] Patel SS, Tirrell M. Annu Rev Phys Chem 1989;40:597.
[8] Milner ST, Witten TA, Cates ME. Macromolecules 1988;21:2610;
Milner ST. Science 1991;252:905.
[9] Semenov AN, Avalos JB, Johner A, Joanny JF. Macromolecules 1996;29: 2179.
[10] Daoulas KC, Theodorou DN, Harmandaris VA, Karayiannis NC, Mavrantzas VG. Macromolecules 2005;38:7134.
[11] Grest GS. Macromolecules 1994;49:5420;
Lai P-Y. Phys Rev E 1994;49:5420;
Daoulas KC, Harmandaris VA, Mavrantzas VG. Macromolecules 2005;38:5780;
Harmandaris VA, Daoulas KC, Mavrantzas VG. Macromolecules 2005;38:5796.
[12] Termonia Y. Polymer 2009;50:1062.
[13] Sanchez IC, Lacombe RH. J Phys Chem 1976;80:2352.
[14] Sanchez IC, Lacombe RH. Polym Lett 1977;15:71.
[15] Sanchez IC, Lacombe RH. Macromolecules 1978;11:1145.
[16] Theodorou DN. Macromolecules 1989;22:4578.
[17] Theodorou DN. Macromolecules 1989;22:4589.
[18] Fleer GJ, Cohen Stuart MA, Scheutjens JM, Cosgrove T, Vincent B. Polymers at interfaces. Cambridge: Chapman and Hall; 1993.
[19] Scheutjens JM, Fleer GJ. J Phys Chem 1979;83:1619.
[20] Scheutjens JM, Fleer GJ. J Phys Chem 1980;84:178.
[21] Cosgrove T, Heath T, van Lent B, Leermakers F, Scheutjens JM. Macromolecules 1988;20:1692.
[22] Evers OA, Scheutjens JM, Fleer GJ. Macromolecules 1990;23:5221.
[23] Fischel LB, Theodorou DN. J Chem Soc Faraday Trans 1995;91:2381.
[24] Terzis AF, Theodorou DN, Stroeks A. Macromolecules 2000;33:1385;
Terzis AF. Polymer 2002;43:2435.
[25] Kritikos G, Terzis AF. Polymer 2005;46:8355.
[26] Kritikos G, Terzis AF. Polymer 2007;48:638.
[27] Wijmans CM, Leermakers FAM, Fleer GJ. J Chem Phys 1994;101:8214.
[28] Kritikos G, Terzis AF. Polymer 2008;49:3601.
[29] Terzis AF, Theodorou DN, Stroeks A. Macromolecules 2000;33:1397;
Terzis AF, Theodorou DN, Stroeks A. Macromolecules 2000;35:508.
[30] Terzis AF. J Phys Conf Ser 2005;10:171.
[31] Termonia Y, Smith P. Macromolecules 1987;20:835.
[32] Mark JE. Physical properties of polymers handbook. WoodBury, New York: American Institute of Physics Press; 1996;
Brandrup J, Immergut EH. Polymer handbook. 3rd ed. New York: John Wiley & Sons; 1989.
[33] Daoud M, Cotton JP. J Phys (Paris) 1982;43:531.
[34] Unpublished experimental and theoretical data.
[35] de Vos Wiebe M, Leemakers Frans AM. Polymer 2009;50:305.
[36] Kovarskii AL. High-pressure chemistry and physics of polymers. New York: CRC Press Inc.; 1994.
[37] Ariyama Takashi, Takenaga Mitsuru. Polym Eng Sci 1992;32:705.
[38] Laurens C, Ober R, Creton C, Leger L. Macromolecules 2004;37:6806;
Laurens C, Creton C, Leger L. Macromolecules 2004;37:6814.